A Computational Strategy for the Theoretical Investigation of the Reactions Between Atomic Oxygen and Aromatic Compounds

Marzio Rosi[1,2(✉)], Nadia Balucani[3], Piergiorgio Casavecchia[2,3], Luca Mancini[3], Giacomo Pannacci[3], and Gianmarco Vanuzzo[3]

[1] Dipartimento di Ingegneria Civile ed Ambientale, Università of Perugia, 06125 Perugia, Italy
marzio.rosi@unipg.it
[2] Istituto CNR di Scienze e Tecnologie Chimiche "Giulio Natta" (CNR-SCITEC), 06123 Perugia, Italy
[3] Dipartimento di Chimica, Biologia e Biotecnologie, Università of di Perugia, 06123 Perugia, Italy
{nadia.balucani,piergiorgio.casavecchia,luca.mancini, giacomo.pannacci,gianmarco.vanuzzo}@unipg.it

Abstract. The theoretical investigation of large aromatic compounds interacting with atomic oxygen is a computationally very challenging problem for the requirements in terms of computer time and scratch disk space. The use of very accurate methods like the CCSD(T) with very extended basis sets is unfeasible. It is necessary to use less expensive methods. In this article we consider a computational strategy able to provide reasonably accurate results with affordable computing costs.

Keywords: Computational chemistry · Density Functional · Theory methods · Coupled Clusted calculations · Complete basis set limit · Potential energy surface

1 Introduction

Aromatic compounds are very common in a plethora of gaseous environments, ranging from combustion systems to planetary atmospheres and the interstellar medium. Their reactions with atomic oxygen can bring to the degradation of the aromatic ring, as already observed in the first detailed studies of the $O(^3P)$ reaction with benzene, pyridine and toluene by some of the present authors [1–4]. More specifically, we took advantage of the versatility of the crossed molecular beam technique with mass spectrometric detection and time-of-flight analysis empowered by the soft ionization approach to measure the experimental branching fractions of the products and infer their reaction mechanism. The interpretation of the experimental results was assisted by electronic structure calculations of the relevant potential energy surface (PES) and kinetics calculations. The results have been surprising and interesting at the same time. Briefly, notable differences have been observed when comparing the reactions with benzene and pyridine

© The Author(s), under exclusive license to Springer Nature Switzerland AG 2024
O. Gervasi et al. (Eds.): ICCSA 2024 Workshops, LNCS 14818, pp. 71–83, 2024.
https://doi.org/10.1007/978-3-031-65273-8_5

(even though they are isoelectronic species for which a similar reaction mechanism was expected) or when comparing the reactions of benzene and toluene (even though the methyl substitution was not expected to affect the reaction mechanism). In particular, the ring contraction channel accounts for ca. 30% of the global yield in the case of the reaction with benzene, 98% in the case of the reaction with pyridine and ca. 10% in the case of the reaction with toluene. In other words, nitrogen in the aromatic ring makes the ring structure more "fragile", while the presence of the methyl group "protects" the ring. The comparison of the experimental branching fractions with the predictions of state-of-the-art quantum calculations proved that the observed differences are due to the different extent of intersystem crossing (ISC) to the underlying singlet PES that, in turn, depends on the coupling terms between the triplet and singlet PESs. Therefore, only an experimental or theoretical characterization of the system will allow us to establish the reaction mechanism and the extent of the ring-contraction channel for any reaction of atomic oxygen with other aromatic compounds.

In our laboratory we are now pursuing a systematic investigation of the reactions of atomic oxygen with other aromatics. In particular, we are interested in characterizing the reaction mechanism for functionalized aromatic compounds, like phenol, anisole, aniline, styrene, etc. to clarify whether the substituent groups are protecting or making more fragile the aromatic ring. We are also interested in the reactions of atomic oxygen with polycyclic aromatic compounds. This knowledge will help to address several issues in applied fields, like for instance the resistance of space technology aromatic polymers or the oxidation of organic compounds in the atmosphere. As already seen in the case of benzene, pyridine and toluene, it is imperative to accompany the experimental work with theoretical predictions. However, theoretical methods become very computationally expensive when the size of the investigated systems increases and their application becomes soon unfeasible. For large systems it is necessary to use less expensive methods. It is necessary, therefore, to check the accuracy of the results and to find a reasonable compromise between the accuracy of the results and the computational cost of the method. The extent of ISC can instead be evaluated by comparing the predictions of the branching fractions in the adiabatic singlet and triplet PESs with the experimental values, as already done in the case of the reactions $O(^3P)$ + HCCCN [5] and $O(^3P)$ + C_2H_3CN [6].

In this contribution we will present a computational strategy to study large systems as those relative to the interaction of atomic oxygen with polycyclic aromatic hydrocarbons or functionalized aromatics and, as examples, we will present the study of the interaction of $O(^3P)$ with toluene and ethylbenzene.

2 Computational Details

The optimization of the stationary points of the Potential Energy Surface (PES) of $O(^3P)$ interacting with toluene and ethylbenzene has been performed at Density Functional Theory (DFT) level of calculation using the ωB97X-D [7, 8] functional, and the 6–311 + G(d,p) basis set [9, 10]. In order to assign the saddle points to the relative reactants and products we performed intrinsic reaction coordinate (IRC) calculations [11, 12]. The energy of all the stationary points of the $O(^3P)$ + toluene system, as well as those

relative to the *ipso* approach of the $O(^3P)$ + ethylbenzene system was computed also at the CCSD(T) level [13–15] using the correlation consistent aug-cc-pVTZ basis set [16] and the ωB97X-D/6–311 + G (d, p) optimized geometries. A similar computational scheme has been previously successfully applied [17–30].

For the stationary points of the $O(^3P)$ + toluene PES, more accurate calculations were performed at the CCSD(T) level corrected with a Density Fitted (DF) MP2 extrapolation to the complete basis set (CBS) and with corrections for core electrons excitations. In particular, we compute the energies as:

$E_{CCSD(T)/CBS}$=E(CCSD(T)/aug-cc-pVTZ)+[E(CCSD(T,core)/cc-pVTZ)-E(CCSD(T)/cc-pVTZ)]+[E(DF-MP2/CBS)-E(DF-MP2/aug-cc-pVTZ)]

where E(DF-MP2/CBS) is defined as:

E(DF-MP2/CBS) = E[(DF-MP2)/aug-cc-pVQZ)] + 0.5772*[E(DF-MP2/aug-cc-pVQZ)-E(DF-MP2/aug-cc-pVTZ)]

The E(DF-MP2/CBS) extrapolation was performed using Martin's two parameter scheme [31]. These energies will be denoted as CCSD(T)/CBS although they include also the core-valence correlation correction. The accuracy of these calculations should be within ± 5 kJ/mol.

For simplicity, in the following discussion the ωB97X-D/6–311 + G(d,p) calculations will be denoted DFT, the CCSD(T)/aug-cc-pVTZ CC and the CCSD(T)/CBS CBS.

All the energies were corrected to 0 K by adding the zero point energy correction computed using the frequencies evaluated at DFT level.

The DFT and CC calculations were done with Gaussian 09 [32] and the CBS calculations with Molpro [33, 34], while the analysis of the vibrational frequencies was performed using Molekel [35, 36].

3 Results and Discussion

3.1 $O(^3P)$ + toluene

The study of the PES of the interaction of atomic oxygen in its ground state (^3P) and toluene has been performed at the DFT level. The choice of the functional is due to the fact that it allows a good description of weak electrostatic adducts, due to the presence of the dispersion term. Moreover, the ωB97X-D functional provides optimized geometries comparable to those obtained with other functionals, like the B3LYP one which describes very well bonding interactions [37]. The whole PES of $O(^3P)$ + toluene has been reported elsewhere [4]. As can be seen from Fig. 1, where we have reported the PES, the approach of $O(^3P)$ to toluene gives rise to a weakly bound van der Waals adduct. The attack of oxygen to the aromatic ring gives rise to four different isomers, since the oxygen atom can approach the ring in *ipso*, *ortho*, *meta* and *para* sites. In the upper panel of Fig. 1, we have reported the reaction pathway arising from the *ipso* attack of oxygen, while in the lower panel the reaction pathways deriving from the *ortho*, *meta* and *para* approaches of oxygen are reported. The *ipso* approach gives rise to the weakly bound $\mathbf{W1^T}$ van der Waals adduct, which evolves to the more stable $\mathbf{W2^T}$ minimum, through the saddle point $\mathbf{TS1^T}$. $\mathbf{W2^T}$ then dissociates to the products $\mathbf{PR1^T}$, *i.e.* phenoxy and methyl, overcoming

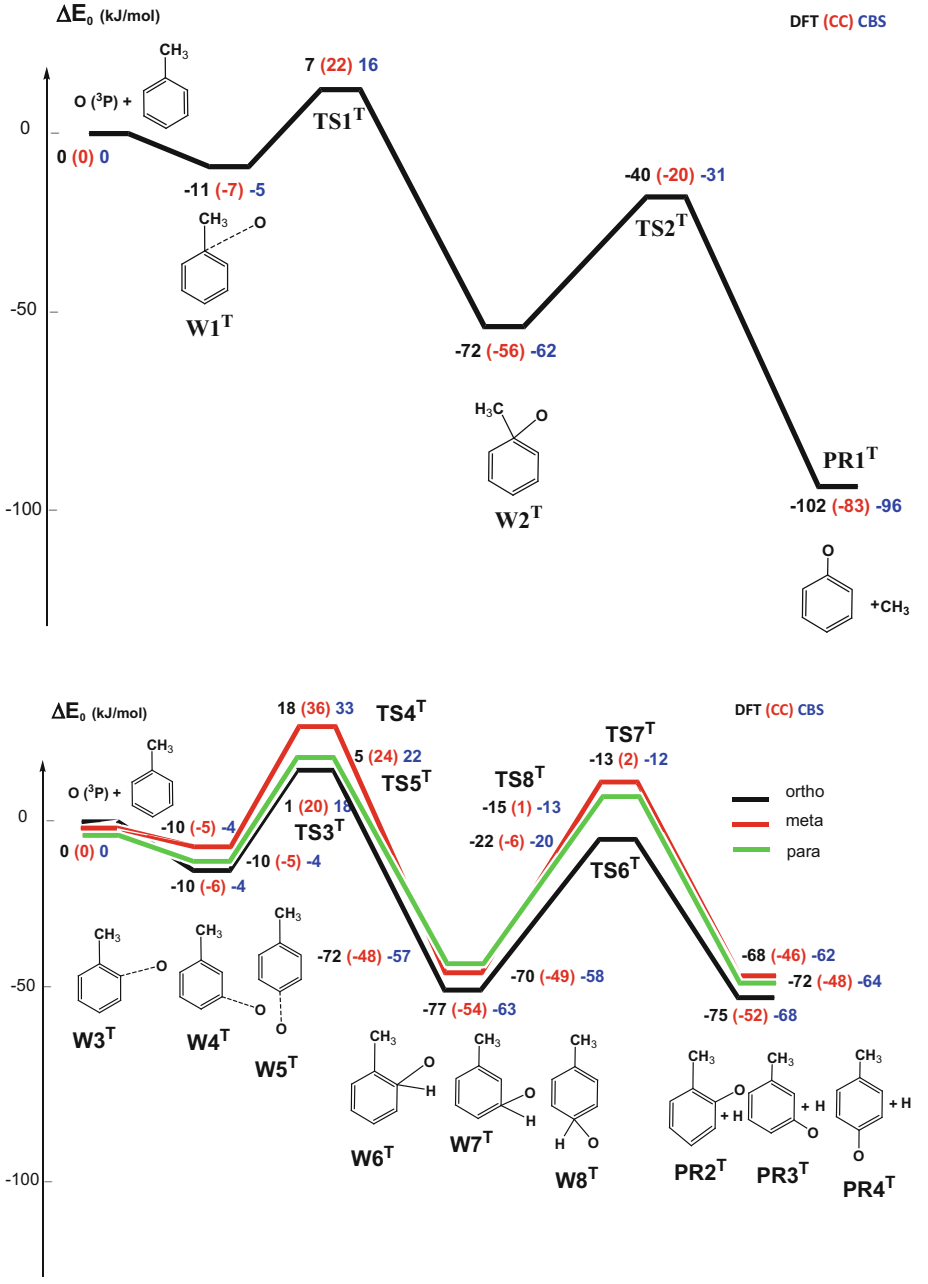

Fig. 1. PES for the O(^{3}P) + toluene reaction. Upper panel refers to the *ipso* attack, while lower panel refers to the *ortho*, *meta* and *para* attacks. Relative energies (kJ/mol) respect to O(^{3}P) + toluene, computed DFT (in black), CC (in red) and CBS (in blue) level. Zero point energy correction always included.

the saddle point **TS2^{T}**. The optimized geometries of the minima are shown in Fig. 2, while the optimized structures of the transition states are reported in Fig. 3. From Fig. 2 we can see that the O-C(*ipso*) distance is very long (2.60 Å) corresponding to a weak electrostatic interaction. This distance becomes 1.61 Å in the saddle point and 1.38 Å in **W2^{T}** suggesting the presence of a chemical bond between C(*ipso*) and O. A similar scenario happens when the oxygen atom approaches the aromatic ring in *ortho*, *meta* or *para* sites (see lower panel of Fig. 1). First of all, we have the formation of a van der Waals adduct which evolves to a stable minimun where a C-O bond is formed. The approach to the *ortho* site is slightly favored with respect to the *para* and *meta* sites, respectively.

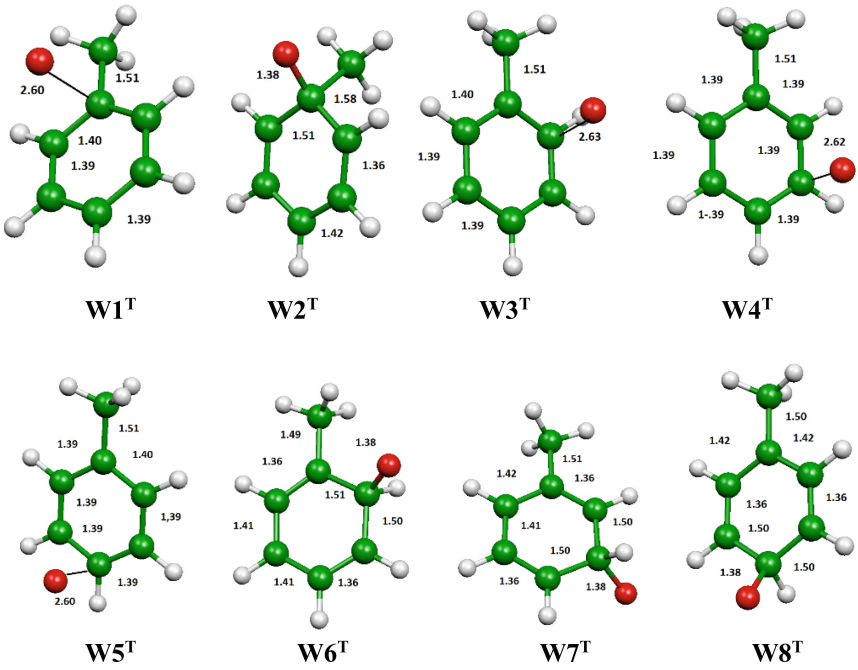

Fig. 2. Optimized geometries of the minima obtained for the attack of O(^{3}P) to toluene, computed at DFT level. Bond lengths in Å, angles in °. The superscript T means toluene.

In order to check the accuracy of the computed energies, we evaluate the relative energies of the stationary points at the DFT level, and then, using the optimized structures, at the CC and at the CBS levels. The relative energies (kJ/mol) with respect to the energy of O(^{3}P) + toluene are reported in Fig. 1; the first value is the DFT relative energy, the second is the CC value, while the third is the CBS value. The ΔE_0 and barrier heights (kJ/mol) for all the reaction steps are reported in Table 1. First of all, we can notice that most of the times the CC energies differ significantly with respect to the most accurate CBS energies. In the CBS method we have included with respect to the CC method a core-valence correlation correction and a correction to extrapolate to the complete basis set limit. Since in our systems we have only first and second period elements, the core-valence correlation correction should be almost negligible, the difference between CC

and CBS should be ascribed almost entirely to basis set superposition errors. This is a bit surprising since the aug-cc-pVTZ basis set is a relatively extended basis set being of triple-zeta quality with polarization and diffuse functions. However, it is well known that the couple cluster method shows a slow convergence on basis set and in order to obtain accurate results it is necessary to use extended basis set. The values reported in Fig. 1 and Table 1 suggest that the aug-cc-pVTZ basis set is far from convergence on basis set limit. The CC results, although computationally very expensive, therefore, show a not negligible basis set superposition error, The DFT results show surprisingly most of the time a better agreement with the CBS results as we can see form Fig. 1 and Table 1. This result could be due in part to the fact that the DFT methods converge rapidly on basis set and even relatively small basis sets provide converged results with respect to basis set. The basis set superposition error therefore should be lower with DFT methods. The ωB97X-D moreover should consider reasonably well also long range interactions due to the presence of the dispersion term. Therefore the DFT approach seems to be able to provide reasonable results at a very low computational cost.

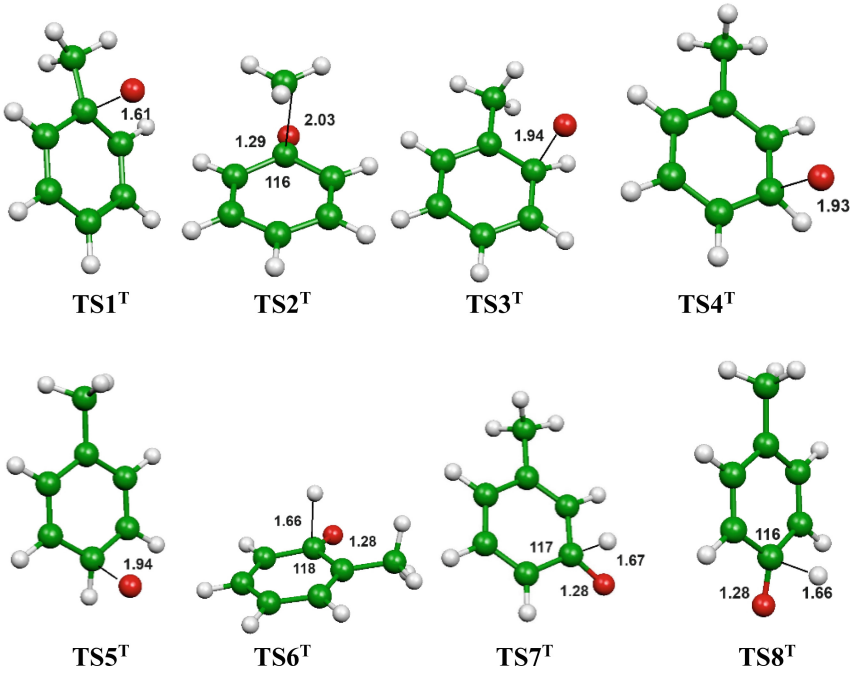

Fig. 3. Optimized geometries of the transition states obtained for the attack of O(^{3}P) to toluene, computed at DFT level. Bond lengths in Å, angles in °. The superscript T means toluene.

3.2 O(^{3}P) + ethylbenzene

The study of the PES of the interaction of atomic oxygen in its ground state (^{3}P) and ethylbenzene has been performed at the DFT level. As can be seen from Fig. 4, where we have reported the PES, the approach of O(^{3}P) to ethylbenzene gives rise to a weakly bound van der Waals adduct. The attack of oxygen to the aromatic ring gives rise to four

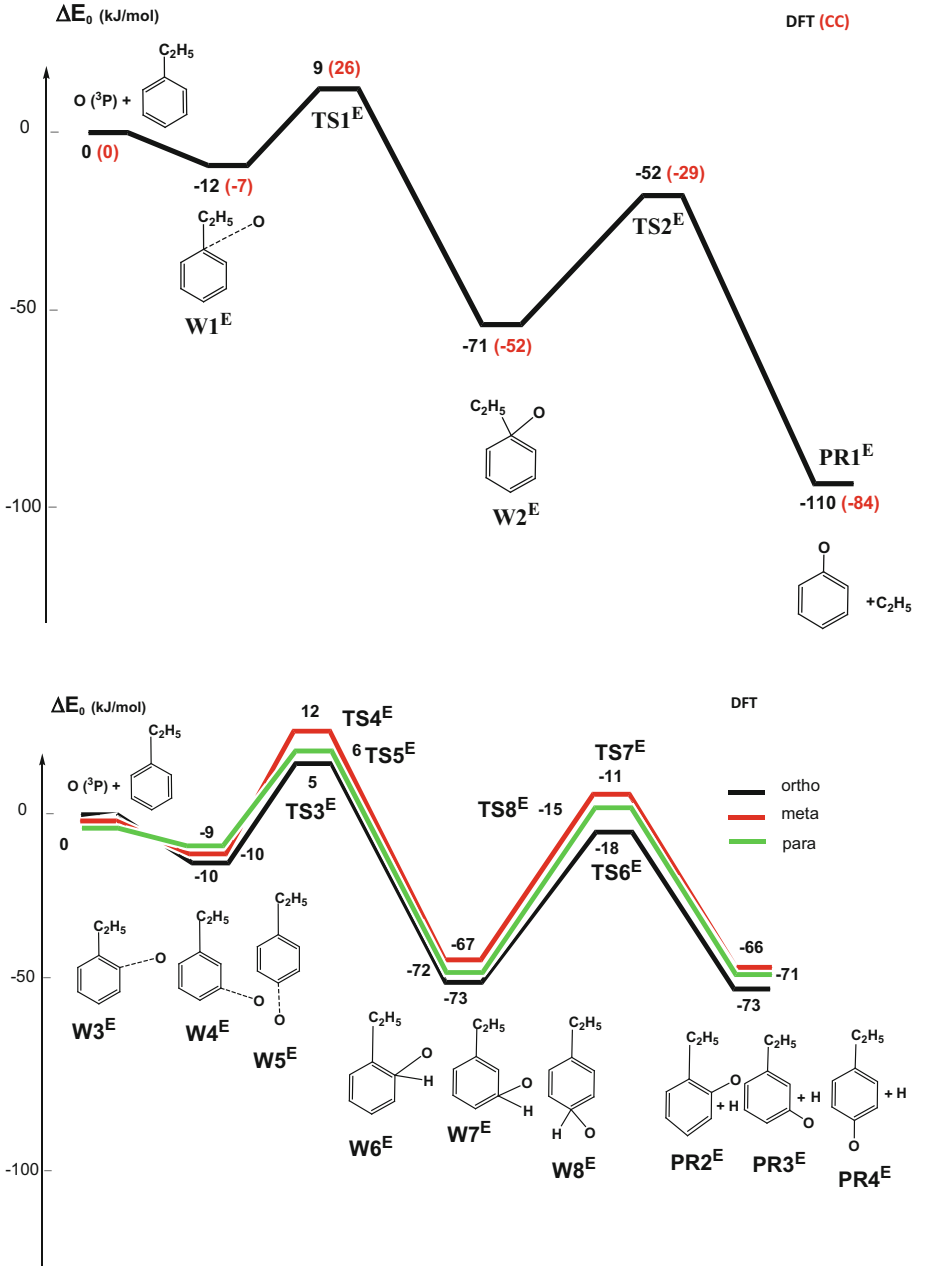

Fig. 4. PES for the O(^{3}P) + ethylbenzene reaction. Upper panel refers to the *ipso* attack, while lower panel refers to the *ortho*, *meta* and *para* attacks. Relative energies (kJ/mol) respect to O(^{3}P) + ethylbenzene, computed at DFT (in black) and CC (in red) level. Zero point energy correction always included.

different isomers, since the oxygen atom can approach the ring in *ipso*, *ortho*, *meta* and *para* sites. In the upper panel of Fig. 4, we have reported the reaction pathway arising from the *ipso* attack of oxygen, while in the lower panel the reaction pathways deriving from the *ortho*, *meta* and *para* approaches of oxygen. The *ipso* approach gives rise to the weakly bound **W1^{E}** van der Waals adduct, which evolves to the more stable **W2^{E}** minimum, through the saddle point **TS1^{E}**. **W2^{E}** then dissociates to the products **PR1^{E}**, *i.e.* phenoxy and ethyl, overcoming the saddle point **TS2^{E}**. The optimized geometries of the minima are shown in Fig. 5, while the optimized structure of the transition states are reported in Fig. 6. From Fig. 5 we can see that the O-C(*ipso*) distance is very long (2.69 Å) corresponding to a weak electrostatic interaction. This distance becomes 1.91 Å in the saddle point and 1.37 Å in **W2^{E}** suggesting the presence of a chemical bond between C(*ipso*) and O. A similar scenario happens when the oxygen atom approaches the aromatic ring in *ortho*, *meta* or *para* sites (see lower panel of Fig. 4). First of all, we have the formation of a van der Waals adduct which evolves to a stable minimun where a C-O bond is formed. The approach to the *ortho* site is slightly preferred with respect to the *para* and *meta* sites, respectively.

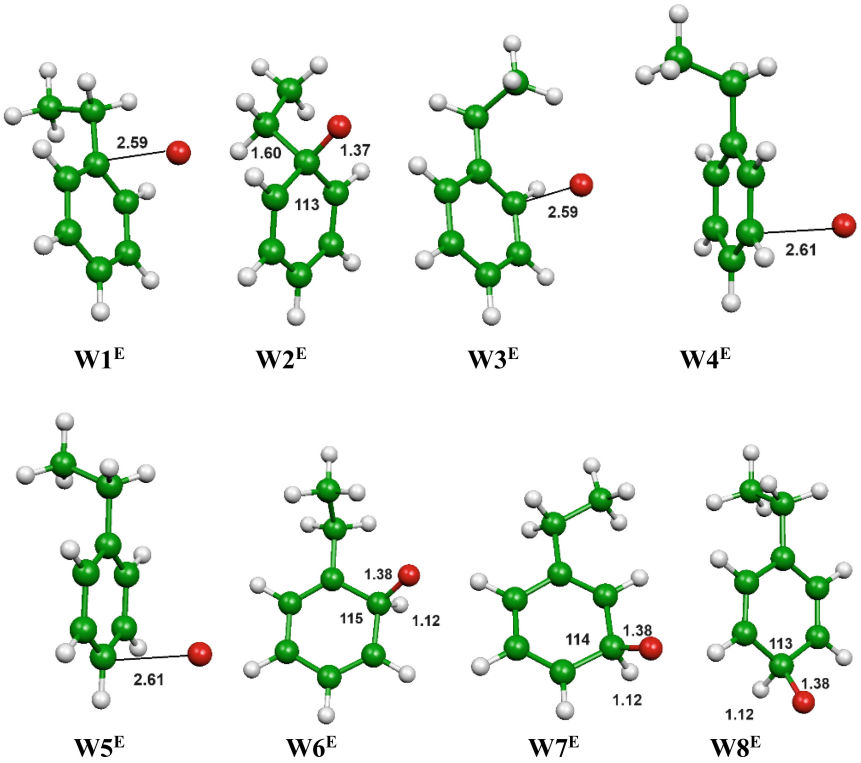

Fig. 5. Optimized geometries of the minima obtained for the attack of O(^{3}P) to ethylbenzene, computed at DFT level. Bond lengths in Å, angles in °. The superscript E means ethylbenzene.

For the reaction pathway relative to the *ipso* approach of the oxygen atom to the ethylbenzene, we have computed the relative energies both at DFT and CC level. The CC calculations were very demanding in terms of computer resources. This effort, however, is probably useless since, due to basis set incompleteness, the CC results are probably less reliable than the DFT values. For this reason for the systems involved in the *ortho*, *meta* and *para* interactions we performed only DFT calculations.

A comparison between the results reported in Fig. 1 and in Fig. 4 suggests that O(^{3}P) + toluene and O(^{3}P) + ethylbenzene systems show a similar behavior as expected for aromatic systems which differ only for the substituent. This comparison however suggests that the DFT method should be adequate also for other aromatic systems interacting with oxygen atoms and, due to its low computational cost, should be feasible also for large polycyclic aromatic compounds.

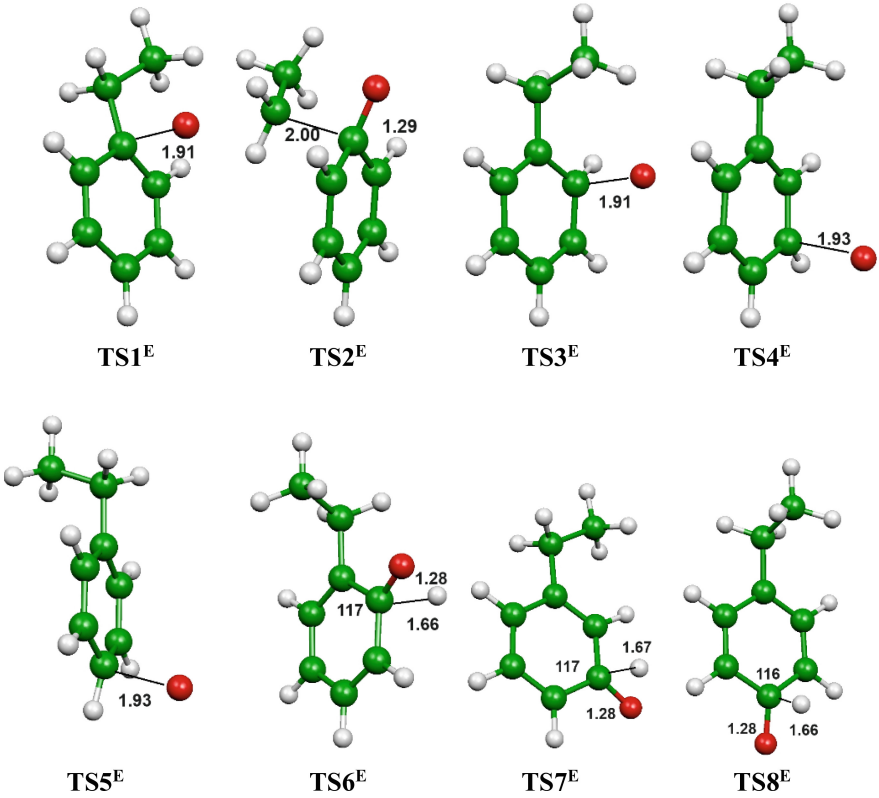

Fig. 6. Optimized geometries of the transition states obtained for the attack of O(^{3}P) to ethylbenzene, computed at DFT level. Bond lengths in Å, angles in °. The superscript E means ethylbenzene.

Table 1. DE_0 and barrier heights (kJ/mol, 0 K) computed at DFT (CC) CBS level for the reaction of $O(^3P)$ with toluene or ethylbenzene. All the energies include zero point energy correction. For the labels of the isomers see Figs. 1 and 4.

	$\Delta E^0{}_0$	Barrier height
$O(^3P)$ + toluene→$W1^T$	−11 (−7) −5	
$W1^T$→$W2^T$	−61 (−49) −57	18 (29) 21
$W2^T$→$PR1^T$	−30 (−27) −34	32 (36) 31
$O(^3P)$ + toluene → $W3^T$	−10 (−6) −4	
$W3^T$ → $W6^T$	−67 (−48) −59	11 (26) 22
$W6^T$ → $PR2^T$	2 (2) −5	35.1 (35.1)
$O(^3P)$ + toluene → $W4^T$	−10 (−5) −4	
$W4^T$ → $W7^T$	−80 (−54) −62	28 (41) 37
$W7^T$→$PR3^T$	2 (3) −4	57 (56) 51
$O(^3P)$ + toluene → $W5^T$	−10 (−5) −4	
$W5^T$ → $W8^T$	−82 (−53) −61	15 (29) 26
$W8^T$ → $PR4^T$	−2 (0) −7	87 (49) 70
$O(^3P)$ + ethylbenzene→$W1^E$	−12 (−7)	
$W1^E$→$W2^E$	−59 (−45)	21 (33)
$W2^E$→$PR1^E$	−39 (−32)	19 (23)
$O(^3P)$ + ethylbenzene → $W3^E$	−10	
$W3^E$ → $W6^E$	−83	15
$W6^E$ → $PR2^E$	0	55
$O(^3P)$ + ethylbenzene → $W4^E$	−10	
$W4^E$ → $W7^E$	−77	22
$W7^E$$PR3^E$	1	56
$O(^3P)$ + ethylbenzene → $W5^E$	−9	
$W5^E$ → $W8^E$	−63	15
$W8^E$ → $PR4^E$	1	57

4 Conclusions

The theoretical study at different level of complexity of the interaction of $O(^3P)$ with toluene and ethylbenzene suggested a computational strategy for the investigation of large aromatic hydrocarbons interacting with oxygen atoms. The study of $O(^3P)$ and toluene has been performed using different methods of increasing complexity, in particular DFT methods with relatively small basis sets, CCSD(T) with a large basis set and CCSD(T) with inclusion of extrapolation to basis set limit. This study suggested that also complex methods like CCSD(T) with large basis sets, as aug-cc-pVTZ, do not

provide very accurate results due to basis set superposition errors. It is necessary to include a correction for basis set incompleteness in order to obtain very accurate results. Simpler methods like DFT, converging much faster on basis set, are able to provide acceptable results at a very low computational cost. These methods have been applied to larger systems as O(^{3}P) interacting with ethylbenzene, where CCSD(T)/CBS calculations are unfeasible with the available computational resources. The same methods can be applied to much larger systems with reasonable costs. This is an important result in order to extend our study to complex PAHs.

Acknowledgments. We acknowledge financial support under the National Recovery and Resilience Plan (NRRP), Mission 4, Component 2, Investment 1.1, Call for tender No. 1409 published on 14.9.2022 by the Italian Ministry of University and Research (MUR), funded by the European Union - NextGenerationEU– Project Title P20223H8CK Degradation of space technology polymers by thermospheric oxygen atoms and ions: an exploration of the reaction mechanisms at an atomistic level (ThermOPoly) - CUP J53D23014440001_- Grant Assignment Decree No. 1386 adopted on 01.09.2023 by the Italian Ministry of Ministry of University and Research (MUR).

We acknowledge financial support under the National Recovery and Resilience Plan (NRRP), Mission 4, Component 2, Investment 1.1, Call for tender No. 104 published on 2.2.2022 by the Italian Ministry of University and Research (MUR), funded by the European Union – NextGenerationEU– Project Title 2022JC2Y93 ChemicalOrigins: linking the fossil composition of the Solar System with the chemistry of protoplanetary disks – CUP J53D23001600006 - Grant Assignment Decree No. 962 adopted on 30.06.2023 by the Italian Ministry of Ministry of University and Research (MUR).

References

1. Cavallotti, C., Pratali Maffei, L., Caracciolo, A., Vanuzzo, G., ìBalucani, N., Casavecchia, P.: Theoretical study of the extent of intersystem crossing in the O(^{3}P) + C_6H_6 reaction with experimental validation. J. Phys. Chem. Lett. **11**(22), 9621–9628 (2020)
2. Vanuzzo, G., et al.: Crossed-beam and theoretical studies of the O(^{3}P, ^{1}D) + benzene reactions: primary products, branching fractions, and role of intersystem crossing. J. Phys. Chem. A **125**(38), 8434–8453 (2021)
3. Recio, P., et al.: Intersystem crossing in the entrance channel of the reaction of O(^{3}P) with pyridine. Nat. Chem. **14**(12), 1405–1412 (2022)
4. Balucani, N., et al.: Crossed molecular beam experiments and theoretical simulations on the multichannel reaction of toluene with atomic oxygen. Faraday Discuss. (2024). https://doi.org/10.1039/D3FD00181D
5. Liang, P., et al.: Reactions O(^{3}P,^{1}D) + HCCCN($X^1\Sigma^+$) (Cyanoacetylene): crossed-beam and theoretical studies and implications for the chemistry of extraterrestrial environments. J. Phys. Chem. A **127**, 685–703 (2023)
6. Pannacci, G., et al.: A combined crossed molecular beam and theorerical study of the O (^{3}P,^{1}D)+ acrylonitrile (CH_2CHCN) reactions and implications for combustion and extraterrestrial environments. Phys. Chem. Chem. Phys. **25**(30), 20194–20211 (2023)
7. Chai, J.D., Head-Gordon, M.: Long-range corrected hybrid density functionals with damped atom-atom dispersion corrections. Phys. Chem. Chem. Phys. **10**, 6615–6620 (2008)
8. Chai, J.D., Head-Gordon, M.: Systematic optimization of long-range corrected hybrid density functionals. J. Chem. Phys. **128**, 084106 (2008)

9. Krishnan, R., Binkley, J.S., Seeger, R., Pople, J.A.: Self-consistent molecular orbital methods. XX. A basis set for correlated wave functions. J. Chem. Phys. **72**, 650–654 (1980)
10. Frisch, M.J., Pople, J.A., Binkley, J.S.: Self-consistent molecular orbital methods 28. Supplementary functions for Gaussian basis sets. J. Chem. Phys. **80**, 3265–3269 (1984)
11. Gonzalez, C., Schlegel, H.B.: An improved algorithm for reaction path following. J. Chem. Phys. **90**, 2154–2161 (1989)
12. Gonzalez, C., Schlegel, H.B.: Reaction path following in mass-weighted internal coordinates. J. Phys. Chem. **94**, 5523–5527 (1990)
13. Bartlett, R.J.: Many-body perturbation theory and coupled cluster theory for electron correlation in molecules Ann. Rev. Phys. Chem. **32**, 359–401 (1981)
14. Raghavachari, K., Trucks, G.W., Pople, J.A., Head-Gordon, M.: Quadratic configuration interaction: a general technique for determining electron correlation energies. Chem. Phys. Lett. **157**, 479–483 (1989)
15. Olsen, J., Jorgensen, P., Koch, H., Balkova, A., Bartlett, R.J.: Full configuration–interaction and state of the art correlation calculations on water in a valence double-zeta basis with polarization functions. J. Chem. Phys. **104**, 8007–8015 (1996)
16. Dunning Jr, T.H.: Gaussian basis sets for use in correlated molecular calculations. I.: the atoms boron through neon and hydrogen. J. Chem. Phys. **90**, 1007–1023 (1989)
17. de Petris, G., Cacace, F., Cipollini, R., Cartoni, A., Rosi, M., Troiani, A.: Experimental detection of theoretically predicted N_2CO. Angew. Chem. **117**, 466–469 (2005)
18. De Petris, G., Rosi, M., Troiani, A.: SSOH and HSSO radicals: an experimental and theoretical study of $[S_2OH]^{0/+/-}$ species. J. Phys. Chem. A **111**, 6526–6533 (2007)
19. Bartolomei, M., et al.: The intermolecular potential in NO-N_2 and $(NO\text{-}N_2)^+$ systems: implications for the neutralization of ionic molecular aggregates. PCCP **10**, 5993–6001 (2008)
20. Leonori, F., et al.: Observation of organosulfur products (thiovinoxy, thioketene and thioformyl) in crossed-beam experiments and low temperature rate coefficients for the reaction $S(^1D) + C_2H_4$. PCCP **11**, 4701–4706 (2009)
21. Leonori, F., et al.: Crossed-beam and theoretical studies of the $S(^1D) + C_2H_2$ reaction. J. Phys. Chem. A **113**, 4330–4339 (2009)
22. De Petris, G., Cartoni, A., Rosi, M., Barone, V., Puzzarini, C., Troiani, A.: The proton affinity and gas-phase basicity of sulfur dioxide. PCCP **12**, 112–115 (2011)
23. Berteloite, C., et al.: Low temperature kinetics, crossed beam dynamics and theoretical studies of the reaction $S(^1D) + CH_4$ and low temperature kinetics of $S(^1D) + C_2H_2$. PCCP **13**, 8485–8501 (2011)
24. Rosi, M., Falcinelli, S., Balucani, N., Casavecchia, P., Leonori, F., Skouteris, D.: Theoretical study of reactions relevant for atmospheric models of Titan: Interaction of excited nitrogen atoms with small hydrocarbons. LNCS **7333**, 331–344 (2012)
25. Skouteris, D., Balucani, N., Faginas-Lago, N., Falcinelli, S., Rosi, M.: Dimerization of methanimine and its charged species in the atmosphere of Titan and interstellar/cometary ice analogs. Astron. Astrophys. **584**, A76 (2015)
26. Salvitti, C., Pepi, F., Troiani, A., Rosi, M., de Petris, G.: The Peroxymonocarbonate anion HCO_4^- as an effective oxidant in the gas phase: a mass spectrometric and theoretical study on the reaction with SO_2 molecules, **28**(1), 132 (2023)
27. Troiani, A., Rosi, M., Garzoli, S., Salvitti, C., de Petris, G.: Vanadium Hydroxide cluster ions in the gas phase: bond-forming reactions of doubly-charged negative ions by SO_2-promoted V-O activation. Chem. Eur. J. **23**, 11752–11756 (2017)
28. Salvitti, C., Rosi, M., Pepi, F., Troiani, A., de Petris, G.: Reactivity of transition metal dioxide anions MO_2^- (M = Co, Ni, Cu, Zn) with sulfur dioxide in the gas phase: an experimental and theoretical study. Chem. Phys. Lett. **776**, 138555 (2021). https://doi.org/10.1016/j.cplett.2021.13855533

29. Troiani, A., Rosi, M., Garzoli, S., Salvitti, C., de Petris, G.: Sulphur dioxide cooperation in hydrolysis reactions of vanadium oxide and hydroxide cluster dianions. J. Chem. **42**(6), 4008–4016 (2018)
30. Troiani, A., Rosi, M., Garzoli, S., Salvitti, C., de Petris, G.: Effective redox reactions by chromium oxide anions: sulfur dioxide oxidation in the gas phase. Int. J. Mass Spectrom. **436**, 18–22 (2019)
31. Troiani, A., Rosi, M., Salvitti, C., de Petris, G.: The oxidation of sulfur dioxide by single and double oxygen transfer paths Chem. Phys. Chem. **15**(13), 2723–2731 (2014)
32. Martin, J.M.: Ab initio total atomization energies of small molecules — towards the basis set limit. Chem. Phys. Lett. **259**, 669–678 (1996)
33. Frisch, M.J., et al.: gaussian 09. In: Gaussian. Inc., Wallingford CT, vol. 121, pp. 150–166 (2009)
34. Werner, H.J., Knowles, P.J., Knizia, G., Manby, F.R., Schütz, M.: Molpro: a general-purpose quantum chemistry program package. WIREs Comput. Mol. Sci. **2**, 242–253 (2012)
35. Werner, H.J., et al.: The Molpro quantum chemistry package. J. Chem. Phys. **152**, 144107 (2020)
36. Flükiger, P., Lüthi, H.P., Portmann, S., Weber, J.: MOLEKEL 4.3, Swiss Center for Scientific Computing, Manno. In: An Interactive Molecular Graphics Tool, vol. 54, pp. 766–769, Chimia, Switzerland (2000)
37. nn, M., et al.: A computational study of the reaction between N(^{2}D) and simple aromatic hydrocarbons. LNCS **14105**, 718–734 (2023)